Spontaneous and Inductive Thickenings of Lamellar Crystal Monolayers of Low Molecular Weight PEO Fractions on Surface of Solid Substrates†

Xue-Mei Zhai, Wei Wang,* Zhen-Peng Ma, Xiao-Jing Wen, Fei Yuan, Xiong-Feng Tang, and Bing-Lin He

Key Laboratory of Functional Polymer Materials for Adsorption and Separation and Institute of Polymer Chemistry, College of Chemistry, Nankai University, Tianjin 300071, China

Received October 31, 2004; Revised Manuscript Received December 7, 2004

ABSTRACT: Crystalline macromolecules form folded-chain lamellar and metastable crystals. Annealing at a temperature below melting point results in a thickening of the metastable crystals to construct more stable ones. Such a process was visualized by AFM equipped with a hot stage in monolayers of poly(ethylene oxide) lamellar crystals on a silicon wafer surface. Our observations show that the monolayers can be thickened in a stepwise manner during stepwise heating to temperatures below the melting point. Our analyses show the thickening process and mechanism as follows: At the first step a small portion of the lamellar crystals have the capability to be spontaneously thickened into a thicker one at a certain temperature range, giving rise to a difference in lamellar thickness. In the following step the thinner lamellae are forced to melt, and then the melted molecules enter an amorphous phase in which they are transported toward the thicker lamellae and finally recrystallize in the thicker ones. This inductive mechanism is analogous to the evaporation−condensation mechanism.

Introduction

Because of their long chain nature, crystallization and melting of linear macromolecules are highly complex processes in comparison with small molecules.[1−6] Under the supercooling condition macromolecules kinetically prefer to be folded several times to form folded-chain (FC) lamellar crystals, of which thickness is normally less than the contour length of molecules. However, the thermodynamically equilibrium state of the lamellar crystals is reached only when extended-chain (EC) lamellae are formed, meaning that FC lamellae are morphologically metastable.[5] Therefore, the number of folds or the thickness of FC lamellae will depend highly on the crystallization condition. In the past decades small-angle X-ray scattering (SAXS), differential scanning calorimetry (DSC), and polarized light microscopy (PLM) are the methods to study the crystallization and melting processes occurring in bulk samples. Recently, using an atomic force microscope (AFM) equipped with a hot stage allows to visualize in real space and to trace in real time crystallization and melting of thin film specimens.[7−10] The results obtained do help us have a better understanding of the molecular mechanism.

Thickening of FC lamellae is an intriguing ordering process which has been intensively studied experimentally and theoretically in the past decades.[11−38] Polyethylene (PE) and poly(ethylene oxide) (PEO), in particular their low molecular weight fractions with mono or narrow mass distribution,[6] have been highly focused on. SAXS, DSC, PLM, and Raman spectrometry are the methods used frequently to follow the thickening process. There are two main mechanisms that have been proposed to explain the thickening process. One of them is the sliding motion mechanism in which molecules in thinner lamellae are suggested to migrate to adjacent lamellae via sliding motion.[15,18,22−25,27−29,31] According to this mechanism, the thickness of the thickened lamellae is normally doubled. Melting−recrystallization is another important mechanism which emphasizes melting of thinner lamellae and then recrystallization into thicker lamellae.[12,13,16,25,26,31] Recently, AFM has been also employed to the thickening process of PE single crystals[35,36] and PEO lamellar crystals in bulk samples.[31] Unfortunately, these works cannot provide more details of the thickening process as well as the mechanism. Accordingly, we are still far from a complete understanding of the molecular mechanism mainly because of a lack of actually characterizing the thickening process.

The first-order transition of binary systems is one of important topics of condensed matter physics when rapidly quenched from a one-phase, thermal equilibrium state to a one-phase, nonequilibrium state.[39−41] Such a quenched system then gradually develops from this nonequilibrium state to an equilibrium thermodynamic state that consists of two coexisting phases. When the system consists of a minority phase in droplet form suspended in a supersaturated phase, Lifshitz and Slyozov[42] and Wagner[43] derived a famous theory to describe the growth dynamics of droplets at a late stage. Assuming that droplets are sufficiently large and with low mobility, the physics of this late stage growth is that droplets, larger than a critical size, will grow by absorbing material from droplets having a size smaller than the critical size until they are finally dissolved; that is an evaporation−condensation mechanism. The driving force is to minimize the interfacial free energy between two phases. Such a growth and coarsening process is normally called Ostwald ripening.[44,45]

In this work, we will report our experimental study regarding the thickening process of a monolayer of PEO lamellar crystals on a silicon wafer surface obtained by AFM in real space. Our observations indicate that the thickening process should be divided into two steps: At the first step a small portion of the lamellar crystals

† Dedicated to Prof. Dr. Gerhard Wegner on the occasion of his 65th birthday.

* To whom correspondence should be addressed. E-mail: weiwang@nankai.edu.cn.

10.1021/ma047764+ CCC: $30.25
Published on Web 02/03/2005

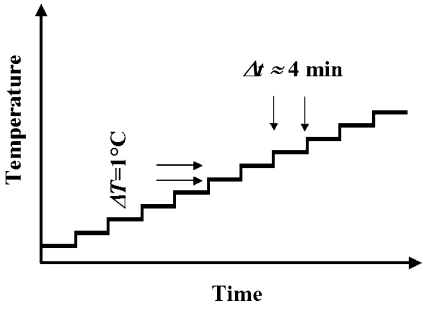

Figure 1. Experimental conditions used during AFM measurements.

have the capability to be spontaneously thickened into a thicker one at a certain temperature range, giving rise to a difference in lamellar thickness. And then, they will force the thinner lamellae to melt and then to recrystallize in the thicker ones. In other words, these thinner lamellae are inductively thickened. We will emphasize that the process is a typical Ostwald ripening,[44,45] and the mechanism of the inductive thickening is analogous to the evaporation−condensation mechanism.[42,43] Most significantly, this is the first time that such a mechanism can be employed to the systems composed of the crystals with high anisotropy in surface tension.

Experimental Part

In this work we selected a poly(ethylene oxide) (PEO) with a low molecular weight ($\bar{M}_n$ = 5000 g/mol) and a narrow molecular weight distribution ($\bar{M}_w/\bar{M}_n$ = 1.05) as the model system. This is because this PEO may form lamellae of thickness l, which is always an integer submultiple of the total chain length L, $l(n) = L/(n + 1)$, where n is the number of folds (quantized folding).[11,14] The polymer used was purchased from Fluka. The maximum length of the molecules in the fully extended form is $L = l_m N = 31.6$ nm.[20]

To visualize in real space and to track in real time the thickening process of PEO lamellar crystals, we used an atomic force microscope (Digital Instrumental Nanscope IV) equipped with a hot stage and a temperature controller with which the temperature can be precisely controlled to ±0.1 °C. All measurements were performed in a tapping mode. The conditions used in our in-situ measurements are to heat the samples from room temperature to the melting temperature of this PEO, as schematically shown in Figure 1. The temperature increment is 1 °C. At each temperature one scan was performed which could be completed within about 4 min. The temperature preset and the height measured were calibrated using the standard samples provided by Digital Instruments.

The samples were prepared as follows: The toluene solutions with a concentration of 0.01−0.02 wt % were prepared in glassware. The silicon wafers were cleaned in an ultrasonic water bath and then in an acetone bath. The thin PEO films on the surface of the silicon wafers were prepared simply by dropping the polymer solution at room temperature. The samples were dried at normal atmosphere overnight and then were treated in a vacuum oven at room temperature for 12 h. Our AFM measurement shows a monolayer of lamellar crystals with fractal-like patterns on the surface of the silicon wafers through diffusion-limited aggregation.[37,38]

Results and Discussion

Crystal Patterns of Fresh Samples. Following our specimen preparation method mentioned above, fractal-like patterns, formed by lamellar crystals of PEO, appear on the surface of the silicon wafers, as shown by the AFM height and amplitude images in Figure 2. Clearly, the pattern shown in Figure 2 is similar to those reported in refs 37 and 38 although different sample preparation methods were used. This means that the same diffusion-limited aggregation mechanism[46] creates a similar pattern. Differently, we can create such a pattern on the whole surface of the wafer. The measured thickness of the lamellar crystals is normally between 6 and 7 nm, so the chains are folded about 4−5 times. Most importantly, it is a *monolayer* of the lamellar crystals that lies on the wafer surface with a free surface, as demonstrated by a three-dimensional image in Figure 3, which shows an enlarged part of the fractal-like crystals. The *c*-axis of the crystals is perpendicular to the wafer surface or parallel to the thickening direction.[37,38] So, such specimens are ideal for studying the thickening process of macromolecular crystals by AFM.

Change of Crystal Pattern with Temperature. The change in pattern of monolayers, which is shown in Figure 3, with temperature (in a range of 24−62 °C)

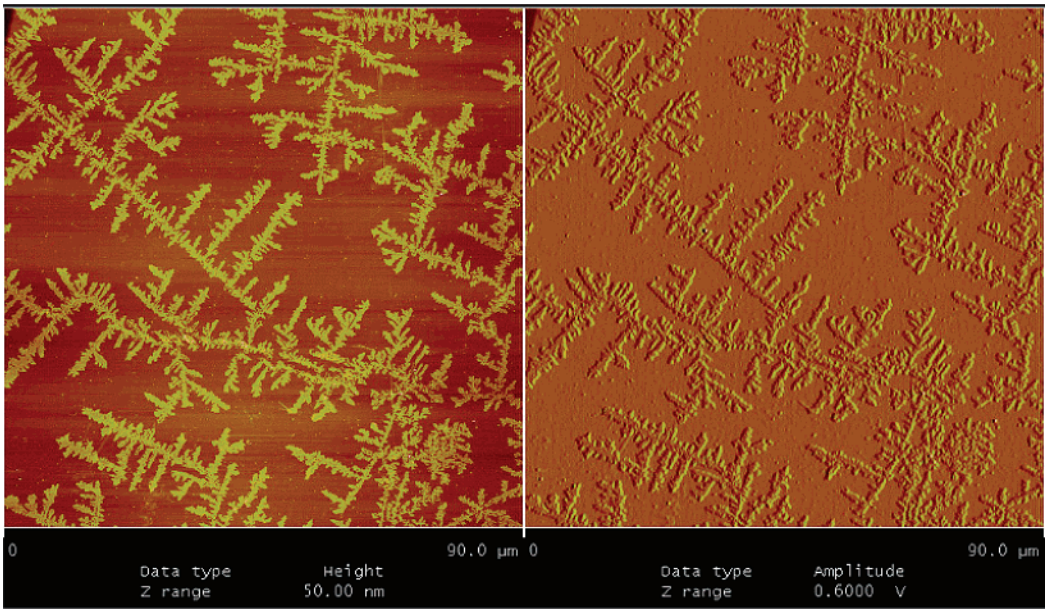

Figure 2. AFM height and amplitude images showing the fingerlike pattern of a monolayer of PEO crystals on the silicon wafer surface. This sample was prepared by dropping a dilute solution of PEO in toluene on the silicon wafer surface.

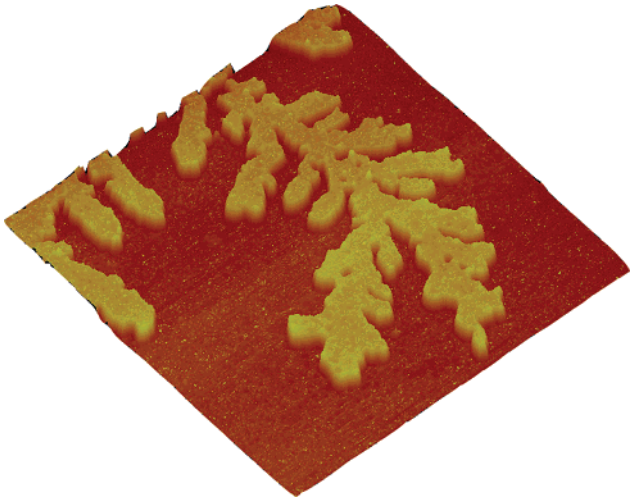

Figure 3. Three-dimensional height image showing a monolayer on the silicon wafer surface.

was shown by the 12 selected height images in Figure 4. These images along with many others (not shown here), which were taken from the same area, evidently present a clear picture of the variations of the monolayer in shape, size in $x-y$ plane, and height (or thickness) in the z-direction when the temperature gradually increases to 62 °C, the melting point of this PEO. The entire process started with a gradual loss of the connectivity of the fractal-like pattern at about 34 °C to form several isolated fragments with irregular shapes (see images a−d). This is a typical process relating to the fragmentation of two-dimensional fractals.[47−49] In images a and b we can see pronounced rims which are slightly higher than the crystals in the internal areas. This slight difference in height produces disappearance of the internal crystals, so the fragments are with some holes at first (see image b) and then more irregular in shape (see images c and d). The further increase of the temperature caused an obvious change of irregularly shaped fragments into round-shaped islands (see images e and f) and then an reduction of the island number (see images f to d). Normally, the size of most islands was gradually shrinking, except the one pointed out by arrow D. As demonstrated by images j to l, its size reduced upon 60 °C and disappeared at 62 °C. (After determining the thickness, we found that this is the equilibrium melting temperature.) To easily study the process and mechanism of the PEO monolayer, we focus on four areas as pointed out by the arrows A to D.

Change of Sizes of Total Area and Some Isolated Islands. The temperature dependence of the total area, A, of the crystals and its differential, dA/dT, are shown in Figure 5. The total area continuously decreases with increasing temperature in a stepwise manner, indicating a stepwise melting of most relatively thinner crystals. The four peak temperatures of the differential curve correspond to the four thickening temperatures, T_{th}^{total}, reflecting an average change of the four thickening processes. They are 34, 42, 48, and 55 °C, respectively. Figure 6B−D shows the area change of the three isolated islands B to D. The area B shrinks and disappears at 45 °C. The area C shrinks slightly before 42 °C, keeps at a constant to 47 °C, and then grows from 47 to 52 °C. Starting at 52 °C, its area decreases considerably and becomes zero at 57 °C. For area D its area increases with different rates before 60 °C. From the figure we can see the rate is speeded up twice at 50

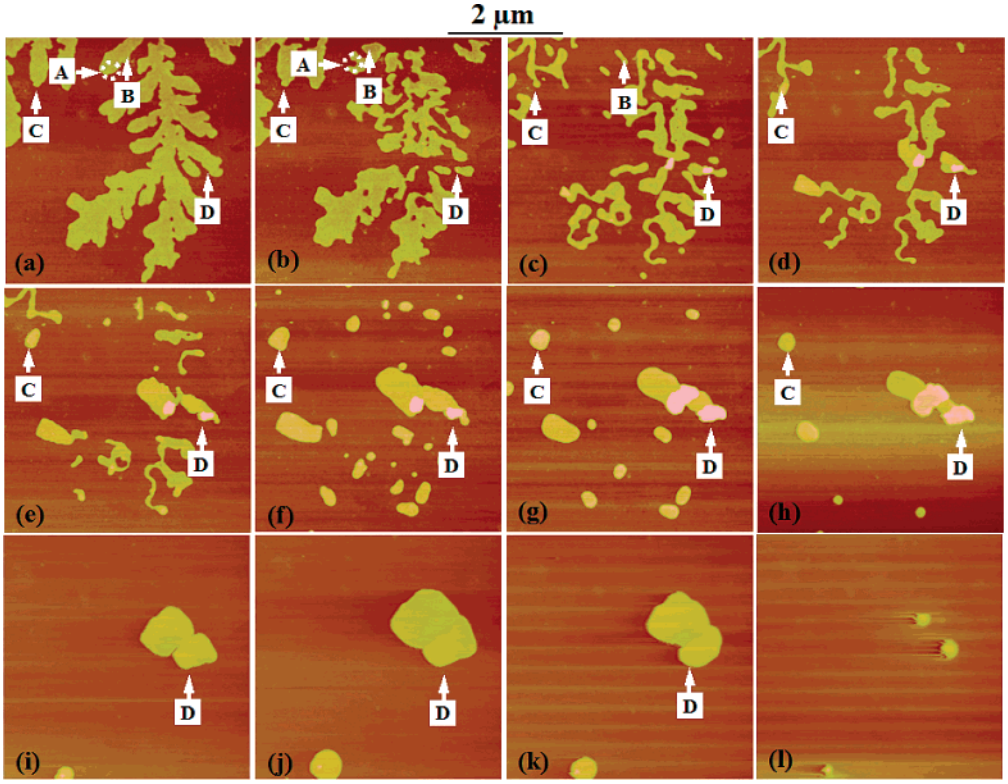

Figure 4. AFM height images showing the variations of PEO lamellar crystals with increasing temperature. The scale in z-direction is 40 nm for (a) to (h) and 100 nm for (i) to (l). The corresponding temperatures are 31 °C for (a), 35 °C for (b), 44 °C for (c), 48 °C for (d), 49 °C for (e), 51 °C for (f), 55 °C for (g), 56 °C for (h), 57 °C for (i), 60 °C for (j), 61 °C for (k), and 62 °C for (l). Arrows A to D point out the areas of which size and height were measured.

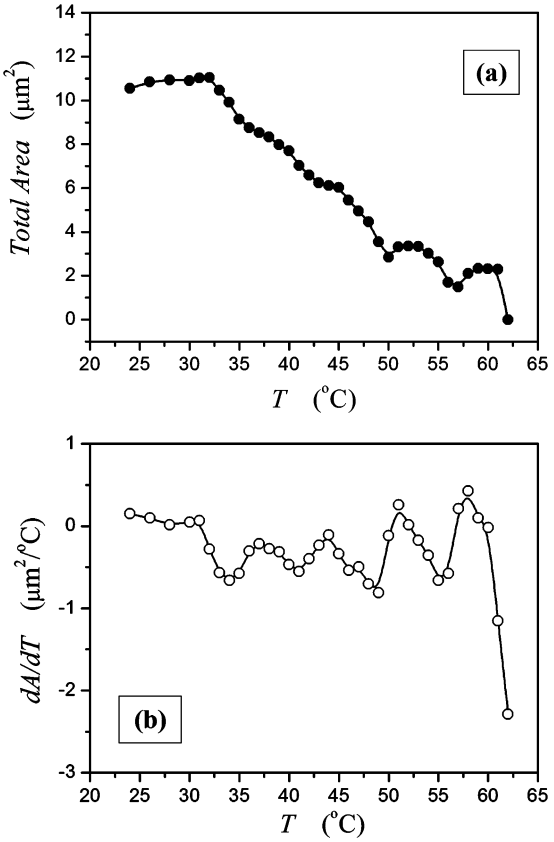

Figure 5. Temperature dependences of the total area, A, of the PEO crystals (a) and its differential to temperature, dA/dT (b). The error is smaller than ±100 nm^2.

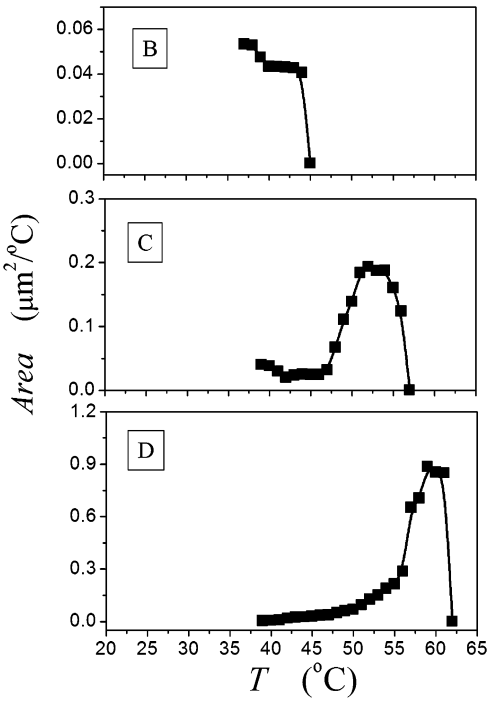

Figure 6. Temperature dependences of the three selected areas B to D. The error is smaller than ±100 nm^2.

and 55 °C. It vanishes dramatically shortly before the equilibrium melting point of this PEO sample.

Changes of Height and Volume. The thickening process is reflected by the height change of the PEO monolayer. So, the heights of the crystals were carefully measured, and their change with temperature was

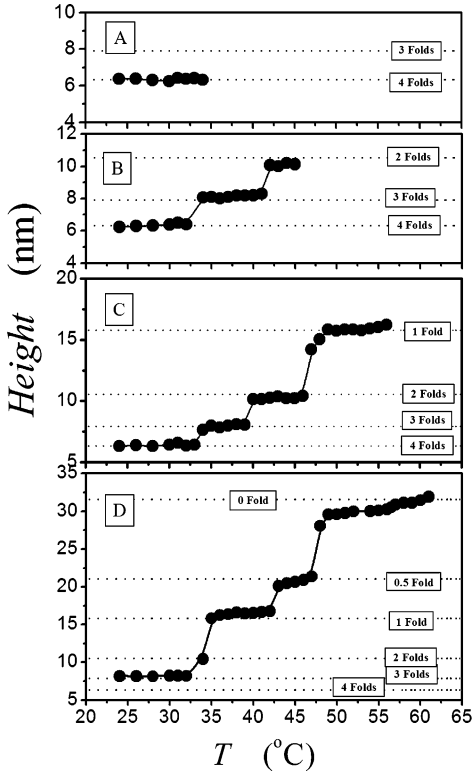

Figure 7. Typical height variations with temperature for the four selected areas. The dotted lines mark the lamellar thicknesses of the crystals with different folds. The error is smaller than ±1 nm.

carefully analyzed accordingly. At the same time we measured the volume of the isolated islands (or fragments) and the volume change with temperature. In this work we found that the average height measured cannot correctly reflect the thickness variation of the crystals because some crystals melt and then disappear, while others are thickened. Therefore, we select the four typical areas with a typical size about 250 nm × 250 nm, as also pointed out by arrows A to D in Figure 4a, to track their thickness variation, as shown in Figure 7. The dotted lines show the thickness of the crystals with different integer folds.

The monolayers in the areas A to C (and most areas in Figure 3a) have an initial thickness about 6.3 nm, meaning a 4-time fold. With increasing temperature to 35 °C the monolayer in the area A suddenly disappears, as shown in Figure 7A. The monolayer in area B, nearby area A, is thickened at 33 °C from 6.3 nm (4 folds) to 7.8 nm (3 folds) and at 42 °C to 10.5 nm (2 folds) (Figure 7B). But, its size is reduced in the interval of 36−45 °C. Its volume change, $\Delta V(45-36) \approx 0$ nm^3, indicates that melted molecules are reused by its own to build up a thicker crystal until it finally disappears at 45 °C.[50] The height variation of area C is totally same as that of area B. The thickening occurs at 35 °C from 6.3 to 7.8 nm, at 39 °C to 10.5 nm, and at 46 °C to 15.8 nm (1 fold). Its size slightly decreases from 37 to 42 °C, remains unchanged from 42 to 47 °C, dramatically increases from 47 to 52 °C, and finally dramatically decreases from 52 to 56 °C. At 56 °C it dissolves. The corresponding volume changes are as follows: $\Delta V(43-39) = -6.5 \times 10^4$ nm^3, $\Delta V(46-43) \approx 0$ nm^3, $\Delta V(51-46) = 2.6 \times 10^6$ nm^3, $\Delta V(54-51) \approx 0$ nm^3, and $\Delta V(54-57) = -2.9 \times 10^6$ nm^3. These illustrate that at the thickening from 7.8 to 10.5 nm this fragment loses material,

Table 1. T_{th} Detected from Areas A to B and the Total Area

$N \rightarrow n-1$	T_{th}^{A} (°C)	T_{th}^{B} (°C)	T_{th}^{C} (°C)	T_{th}^{D} (°C)	T_{th}^{total} (°C)
4→3		32	33		34
3→2		42	39	32	42
2→1			47	34	48
1→0.5				43	
0.5→0				47	55

but at the thickening from 10.5 to 15.8 nm it gains a great amount of material from the thinner and melting crystals around. Above 54 °C it fails the competition with another stronger competitor(s) so it loses its material completely.

Area D has an initial thickness of 7.8 nm, which corresponds to a 3-time fold, 1 fold less than the other areas. Because of this innate superiority, its thickening takes place at 32 °C from 7.8 to 10.5 nm, at 34 °C to 15.8 nm, at 43 °C to 21.1 nm, and at 47 °C 31.6 nm (the EC crystals) (see Figure 7D). Its size slowly increases from 37 to 55 °C, then rapidly increases until 60 °C, and finally reduces rapidly. In the interval of 55−60 °C $\Delta V \approx 2.0 \times 10^7$ nm^3. Above 60 °C only two crystals with a thickness of 31.6 nm can survive in the frame scanned until the melting point (62 °C). Their volume is about 6.9×10^7 nm^3, approximately equal to the volume of the PEO film at 30 °C, further meaning that all molecules in the scanned frame are absorbed by them.

Thickening Temperature and Spontaneous Thickening (ST) Mechanism. In this work we define a thickening temperature T_{th} showing that the PEO crystals can be *spontaneously* thickened from n to $(n-1)$ folds (see Figure 7). Table 1 summarizes T_{th} of the areas A to D and measured from the variation of the total area. Clearly, we can derive an inequality as

$$T_{th}^{D} < T_{th}^{C} < T_{th}^{B} < T_{th}^{total} \quad (1)$$

for the same thickening steps, illustrating that the crystals in areas B to D can be spontaneously thickened to 10.5 nm during the competition with crystal A and many others. Meanwhile, in the competition between crystals B to D, crystals C and D beat crystal B at the step to 15.8 nm. Likewise, crystal D beats crystal C at the step to 31.6 nm. In conclusion, the crystals having the lower spontaneously thickening temperature will be able to stand in the further competition.

Now we can understand why the growth rate of the crystal D is speeded up twice at 50 and 55 °C (see Figure 4D). At the temperature range below 50 °C, crystal D with some other ST crystals beat many thinner crystals and shared the material lost by these thinner crystals. In the temperature range between 50 and 55 °C, the number of the crystals, which have been spontaneously thickened so can share the lost material with crystal D, becomes less because some former thicker crystals cannot be spontaneously thickened at this step. So crystal D can absorb more materials, and its growth rate is increased. Upon 55 °C, crystal D with another one in the scanned frame becomes the crystals that can be thickened to EC crystal. So, they plunder all material from other crystals with a higher growth rate.

Summary of the Physical Processes. In Figure 8 we summarize the processes that occurred when heating the sample from room temperature to equilibrium temperature. Under the conditions used, the lamellar crystals are gradually thickened in the temperature range from room temperature to 60 °C. On average the thickening processes from 4 to 3 folds, 3 to 2 folds, 2 to 1 fold, and 1 to 0 fold occurred at about 34, 42, 48, and 55 °C, respectively.[51] In the temperature range from 25 to about 44 °C, the main process is the fragmentation of the fractal-like pattern, while the Ostwald repining occurs in the range from 44 to 60 °C. The thickening of the lamellar crystals causes these processes. At 60 °C the lamellar thickness attains the EC thickness. Our determination shows the same volume at 25 and 60 °C, giving rise to an indication that this system is a conserved one. Further increasing temperature to 62 °C will cause melting of the EC lamellar crystals, so the equilibrium melting point of this sample is about 62 °C.

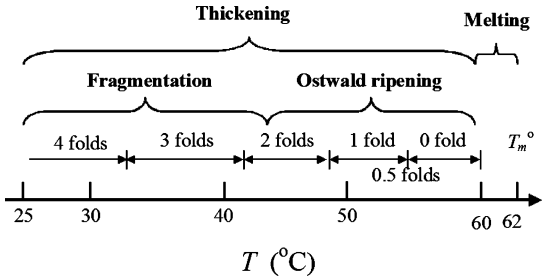

Figure 8. Summary of the physical processes happened during heating the sample to 62 °C.

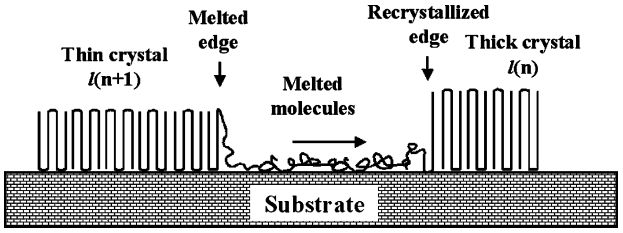

Figure 9. Schematic representation of process and molecular mechanism occurring in inductive thickening of this system.

Inductive Thickening (IT) Mechanism and Evaporation−Condensation Mechanism. So far we have demonstrated that at each thickening step only a small portion of lamellar crystals can spontaneously be thickened. Clearly, a difference in thickness is created. For all thinner crystals their size decrease is clear-cut evidence to indicate these crystals gradually melt and then lose molecules laterally. The quantized thickening and size growth of some spontaneously thickened crystals indicate that they gain molecules from melted crystals to build up more stable crystals. These mean that the thinner crystals are *inductively* thickened. The process may be schematically shown in Figure 9. A very thin amorphous layer[37,38] that should exist on the silicon wafer surface plays a key role in transporting molecules from a thinner lamella ($n+1$ folds) to a thicker lamella (n folds). The mechanism is as follows: The molecules melted from thinner crystals (the order but less stable state) first enter the amorphous layer (disorder state). Then they migrate through the amorphous layer toward the thicker crystals, and are finally absorbed by and recrystallized in the thicker crystals (order and more stable state). At a certain temperature there must be a critical thickness, corresponding to a certain melting point. The lamellae thicker than the critical value will remain, but thinner than the critical value will dissolve. This mechanism of the inductive thickening is greatly analogous to the evaporation−condensation one[42,43] for the first time observed in a lamellar crystals formed by chain-folding of linear macromolecules.

Conclusion

In summary, our in-situ observations have demonstrated a competition existing in the crystalline polymer systems composed of lamellar crystals with different thicknesses. Once a crystal is *spontaneously* thickened, it becomes thermodynamically more metastable (or stable for EC crystals), and its size may further grow by "plundering" molecules from many thinner crystals until dissolution finally occurs. In other words, the thinner crystals are *inductively* thickened. The molecular mechanism of the inductive thickening process can be described by the evaporation−condensation mechanism. For the first time this mechanism is extended to a system that consists of lamellar crystals with different thicknesses which have different stabilities.

Acknowledgment. We very greatly appreciate Nankai University for a start-up funding and the National Science Foundation of China for a grant (NSFC20474033) to support this work. W.W. thanks for DAAD for a scholarship and the Max-Planck-Institute for Polymer Research (MPI-P) for their hospitality when he completed this manuscript as a visiting scientist at MPI-P.

References and Notes

(1) Bassett, B. C. *Principles of Polymer Morphology*; Cambridge University Press: Cambridge, 1981.
(2) Wunderlich, B. *Macromolecular Physics*; Academic: New York, 1976; Vols. 1 and 2.
(3) Armistead, K.; Goldbeck-Wood, G. *Adv. Polym. Sci.* **1992**, *100*, 219.
(4) Strobl, G. *The Physics of Polymers*, 2nd ed.; Springer: Berlin, 1997.
(5) Keller, A.; Cheng, S. Z. D. *Polymer* **1998**, *39*, 4461.
(6) Ungar, G.; Zeng, X.-B. *Chem. Rev.* **2001**, *101*, 4157−4188.
(7) Pearce, R.; Vancso, G. *Macromolecules* **1997**, *30*, 5843.
(8) Li, L.; Chan, C. M.; Yeung, K. L.; Li, X. J.; Ng, K. M.; Lei, Y. G. *Macromolecules* **2001**, *34*, 316.
(9) Schönherr, H.; Waymouth, R. M.; Frank, C. W. *Macromolecules* **2003**, *36*, 2412.
(10) Xu, J.; Guo, B.-H.; Zhang, Z.-M.; Zhou, J.-J.; Jiang, Y.; Yan, S.; Li, L.; Wu, Q.; Chen, G.-Q.; Schultz, J. M. *Macromolecules* **2004**, *37*, 4118.
(11) Arlie, P.; Spegt, P. A.; Skoulios, A. *Makomol. Chem.* **1966**, *99*, 160; **1967**, *104*, 212.
(12) O'Leary, K.; Geil, P. H. *J. Macromol. Sci., Phys.* **1967**, *B1*, 147.
(13) Mandelkern, L.; Sharma, R. K.; Jackson, J. F. *Macromolecules* **1969**, *2*, 644.
(14) Spegt, P. *Makromol. Chem.* **1970**, *139*, 139.
(15) Dreyfuss, P.; Keller, A. *J. Macromol. Sci., Phys.* **1970**, *B4*, 811.
(16) Fischer, E. W. *Pure Appl. Chem.* **1971**, *26*, 385.
(17) Kovacs, A.; Gonthier, A.; Straupe, C. *J. Polym. Sci., Polym. Symp.* **1975**, *50*, 283.
(18) Pope, D. P.; Keller, A. *J. Polym. Sci., Polym. Phys. Ed.* **1976**, *14*, 821.
(19) Thierry, A.; Skoulios, A. E. *Eur. Polym. J.* **1977**, *13*, 169.
(20) Kovacs, A.; Straupe, C.; Gonthier, A. *J. Polym. Sci., Polym. Symp.* **1977**, *59*, 31.
(21) Kovacs, A.; Straupe, C. *J. Cryst. Growth* **1980**, *48*, 210.
(22) Cheng, S. Z. D.; Zhang, A.-Q.; Barley, J. S.; Chen, J.-H.; Habenschuss, A.; Zschack, P. R. *Macromolecules* **1991**, *24*, 3937.
(23) Ungar, G.; Steiny, J.; Keller, A.; Bidd, I.; Whitting, M. C. *Science* **1985**, *229*, 386.
(24) Phillips, P. J.; Rensch, G. J. *J. Polym. Sci., Polym. Phys. Ed.* **1989**, *27*, 155.
(25) Ichida, T.; Tsuji, M.; Murakami, S.; Kawaguchi, A.; Katayama, K. *Colloid Polym. Sci.* **1985**, *263*, 293.
(26) Cho, M. H.; Kyu, T.; Lin, J. S.; Saijo, K.; Hashimoto, T. *Polymer* **1992**, *33*, 4152.
(27) Yamamoto, T. *J. Chem. Phys.* **1997**, *107*, 2653.
(28) Hikosaka, M.; Amano, K.; Rastogi, S.; Keller, A. *Macromolecules* **1997**, *30*, 2067.
(29) Rastogi, S.; Spoelstra, A. B.; Goossens, J. G. P.; Lemstra, P. J. *Macromolecules* **1997**, *30*, 7880.
(30) Liu, C.; Muthukumar, M. *J. Chem. Phys.* **1998**, *109*, 2563.
(31) Matsuda, H.; Aoike, T.; Uehara, H.; Yamanobe, T.; Komoto, T. *Polymer* **2001**, *42*, 5013.
(32) Beekmans, L. G. M.; van der Meer, D. W.; Vancso, G. J. *Polymer* **2002**, *43*, 1887.
(33) Terry, A. E.; Phillips, T. L.; Hobbs, J. K. *Macromolecules* **2003**, *36*, 3240.
(34) Marand, H.; Huang, Z. *Macromolecules* **2004**, *37*, 6492.
(35) Sanz, M.; Hobbs, J. K.; Miles, M. J. *Langmuir* **2004**, *20*, 5989.
(36) Organ, S. J.; Hobbs, J. K.; Miles, M. J. *Macromolecules* **2004**, *37*, 4562.
(37) Reiter, G.; Sommer, J.-U. *Phys. Rev. Lett.* **1998**, *80*, 3771.
(38) Reiter, G.; Castelein, G.; Sommer, J.-U. *Phys. Rev. Lett.* **2001**, *86*, 5918.
(39) Gunton, J. D.; Miguel, M. S.; Sahni, P. S. In *Phase Transition and Critical Phenomena*; Domb, C., Lebowiz, J. L., Eds.; Academic Press: New York, 1983; Vol. 8, p 367.
(40) Binder, K. *Rep. Prog. Phys.* **1987**, *50*, 783.
(41) Bray, A. J. *Advs. Phys.* **1994**, *43*, 357.
(42) Lifshitz, I. M.; Slyozov, V. V. *J. Phys. Chem. Solids* **1961**, *19*, 35.
(43) Wagner, C. *Z. Elektrochem.* **1961**, *65*, 581.
(44) Ostwald, W. *Z. Phys. Chem.* **1897**, *22*, 289.
(45) Ratke, L.; Voorhees, P. W. *Growth and Coarsening-Ostwald Ripening in Material Processing*; Springer: Berlin, 2002.
(46) Meakin, P. *Fractals, Scaling and Growth Far from Equilibrium*; Cambridge University Press: Cambridge, England, 1997.
(47) Novotnyi, M. A.; Taoi, R.; Landau, D. P. *J. Phys. A.: Math. Gen.* **1990**, *23*, 3271.
(48) Thouy, R.; Olivi-Tran, N.; Jullien, R. *Phys. Rev. B* **1997**, *56*, 5321.
(49) Sharon, E.; Moore, M. G.; McCormick, W. D.; Swinney, H. L. *Phys. Rev. Lett.* **2003**, *91*, 205504.
(50) $\Delta V(T_2 - T_1) = V_{T_2} - V_{T_1}$ means the volume difference between T_1 and T_2.
(51) As presented in Figure 7D, we observed the lamellar crystals showing 0.5 fold. This point will be explained in a further study.

MA047764+